# INORGANIC CHEMISTRY

## FRONTIERS

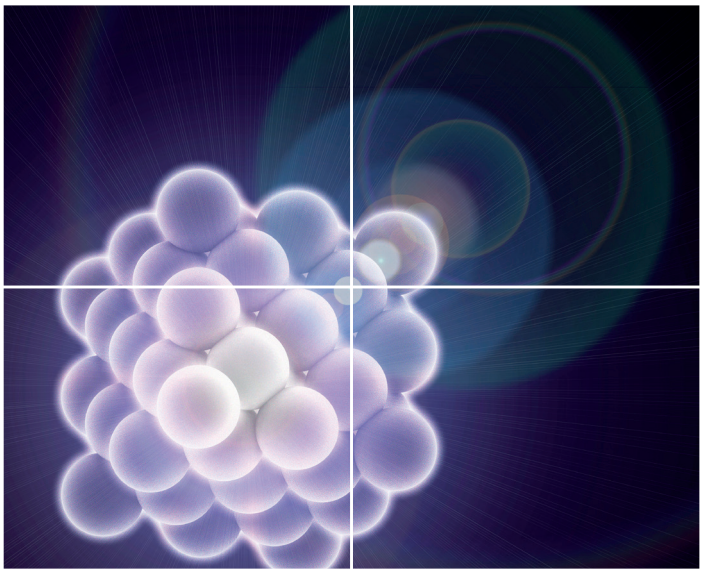

Accepted Manuscript

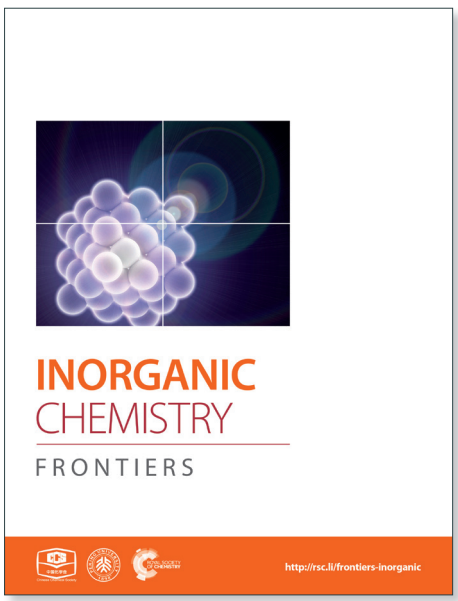


This is an *Accepted Manuscript*, which has been through the Royal Society of Chemistry peer review process and has been accepted for publication.

*Accepted Manuscripts* are published online shortly after acceptance, before technical editing, formatting and proof reading. Using this free service, authors can make their results available to the community, in citable form, before we publish the edited article. We will replace this *Accepted Manuscript* with the edited and formatted *Advance Article* as soon as it is available.

You can find more information about *Accepted Manuscripts* in the **Information for Authors**.

Please note that technical editing may introduce minor changes to the text and/or graphics, which may alter content. The journal's standard **Terms & Conditions** and the **Ethical guidelines** still apply. In no event shall the Royal Society of Chemistry be held responsible for any errors or omissions in this *Accepted Manuscript* or any consequences arising from the use of any information it contains.

## Graphical abstract

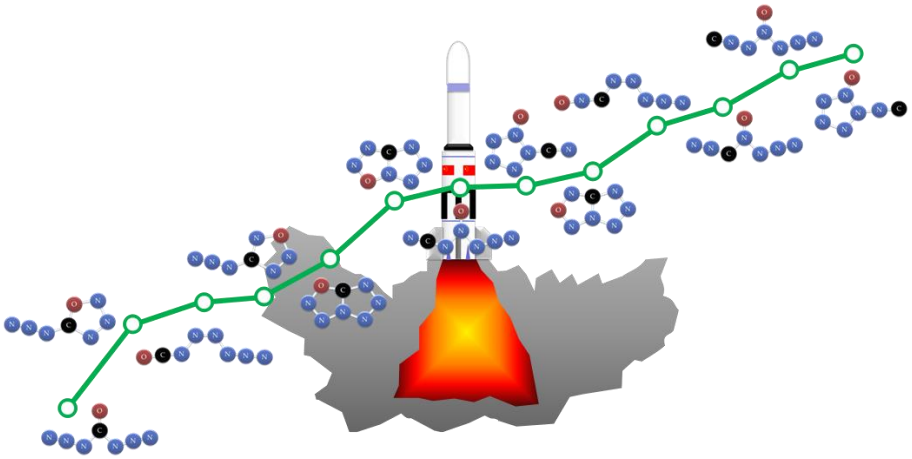

The explored $CN_6O$ isomers are more efficient than carbonyl diazide as rocket fuel.

# A theoretical prediction on $CN_6O$: structure, stability and performance†

Tao Yu[ab] and Bo Wu[*a]

[a]Mutiscale Computational Materials Facility, School of Materials Science and Engineering, Fuzhou University, Fuzhou 350100, P. R. China. E-mail: wubo@fzu.edu.cn; Tel: +86-0591-22866532

[b]Computer-Aided Energetic Materials Design Group, Xi'an Modern Chemistry Research Institute, Xi'an 710065, P. R. China.

† Electronic supplementary information (ESI) available: compounds mapping list for their serial numbers, Kamlet-Jacobs equation, supplementary reaction pathways, barriers of limiting pathways for different isomers of $CN_6O$, gas phase enthalpies of formation for different isomers of $CN_6O$, frontier orbital energies for different isomers of $CN_6O$, enthalpy of formation effect on specific impulse and combustion temperature for $CN_6O$, calculated rocket performances of comparative set (TNT, RDX, HMX, CL-20 and FTDO), molecular volumes for different isomers of $CN_6O$, and calculated detonation performances of comparative set.

The potential energy surfaces of $CN_6O$ isomers were calculated at B3LYP/aug-cc-pVDZ level and the key decomposition pathways were calculated at G3B3 level. The optimum pathway for the decomposition of carbonyl diazide to $OCN_4$ and $N_2$ has a barrier of about 30 kcal $mol^{-1}$. Except for carbonyl diazide, no isomer of $CN_6O$ crosses a higher decomposition barrier than 20 kcal $mol^{-1}$. The specific impulse of carbonyl diazide is close to those of RDX (cyclotrimethylene trinitramine), HMX (cycloteramethylene tetranitramine) and CL-20 (hexanitrohexaazaisowuritane), and the specific impulses of many other $CN_6O$ isomers are greater than that of FTDO ([1,2,5]oxadizolo[3,4-4][1,2,3,4]tetrazine-4,6-di-N-dioxide). The $CN_6O$ system pays a higher combustion temperature than RDX, HMX, CL-20 and FTDO at comparable specific impulses. The detonation velocity and pressure of most of $CN_6O$ isomers are lower than those of CL-20.

## Introduction

Geminal diazides are much more powerful than monoazides and vicinal azides. They are extremely sensitive, explosive, and dangerous either as byproducts or pure substances.[1] Chemical community is interested in these marginally stable compounds. Carbonyl diazide with a sum

formula of $CN_6O$ was synthesized *in situ* by carbonyl dihydrazide, hydrogen chloride, and sodium nitrite in the 1920s.[2,3] Banert *et al.* discovered carbonyl diazide as the hydrolysis product of tetraazidomethane spectroscopically in 2007.[4] Zeng *et al.* synthesized carbonyl diazide *via* the nucleophilic substitution reaction between chlorofluorocarbonyl and sodium azide, the pure compound was firstly isolated and the crystal structure was obtained in 2010.[5] Nolan *et al.* improved the synthetic process using less toxic triphosgene instead of chlorofluorocarbonyl in 2012.[6] The specific energy of carbonyl diazide, decomposition into carbon monoxide and dinitrogen, does not come up to expectation. Compared with the general energetic compounds such as TNT (trinitrotoluene), RDX (cyclotrimethylene trinitramine), and HMX (cycloteramethylene tetranitramine), there is not much difference for the specific energy of carbonyl diazide.[7] In addition, carbonyl diazide has a very common density (1.712 g $cm^{-3}$)[5] which is higher than TNT (1.654 g $cm^{-3}$), but lower than RDX (1.816 g $cm^{-3}$) and HMX (1.910 g $cm^{-3}$).[8]

However, carbonyl diazide possesses some unique characters as rocket fuel or explosive, *e.g.*, high nitrogen content and zero oxygen balance for carbon monoxide. According to Tsiolkovsky[9] and Kamlet-Jacobs[10] equations, the acceleration of single-stage rocket and detonation velocity of explosive depend on combustion energy and density. Unlike explosive, the manufacture of huge or multi-stage rocket may compensate for the loss in fuel density. Thus $CN_6O$ is probably more applicable as rocket fuel than explosive. The most challenge issue for space application is energy content of $CN_6O$, although some other obstacles may bring out in the future.

Most recently, we investigated the $N_7O^+$ cation which is the isoelectronic species of carbonyl diazide, computationally and experimentally, and found that 1-oxo-$N_7O^+$ component is formed in the reaction of $NF_2O^+$ with excess $HN_3$, and 4-oxo-$N_7O^+$ is much more stable than 1-oxo-$N_7O^+$.[11] Both carbonyl diazide and 4-oxo-$N_7O^+$ cation impart W-shape, geminal diazide structure, eight atoms and 56 electrons, but a hetero carbon atom is located at the center of carbonyl diazide chain. As the energy of 1-oxo-$N_7O^+$ is higher than that of 4-oxo-$N_7O^+$ by 18.6 kcal $mol^{-1}$, the atomic arrangements of $CN_6O$ should offer more possibilities due to the replacement nitrogen by carbon.

In this paper, several typical $CN_6O$ isomers were explored by study on the potential surfaces around the electronic structures of different carbon positions in order to increase the energy content, see Fig. 1. The existence of novel $CN_6O$ isomers was demonstrated by geometry optimization, and the stability was estimated by decomposition (or isomerization) barrier. Then we figure out the dependence of structure, enthalpy of formation and stability, and evaluate the potential application of $CN_6O$ as rocket fuel and explosive. The feasibilities presented herein are expected to assist chemists and engineers in molecular design and synthesis.

## Computational methods

The optimized geometries and harmonic frequencies for the reactants, intermediates, transition states and products were calculated using the B3LYP[12,13] method and Dunning's aug-cc-pVDZ[14] basis set. All reactants, intermediates and products have true minima on their potential energy surfaces without any imaginary frequencies, and the transition states have only one imaginary frequency. To check the connection of each transition state, intrinsic reaction coordinate (IRC)[15,16] calculations were carried out. The correlative energies of key pathways were also calculated at the composite G3B3 level[17,18] (a G3 variant using B3LYP geometries). The standard enthalpies of formation were calculated by atomic method which the target compounds are formed from their

constituent atoms in gas phases. The experimental atomic enthalpies were referred from NIST Chemistry Web book.[19] The free energy activation barriers were derived by the differences between transition states and reactants (or products) at 0 and 298.15 K, respectively. Numbering schemes for the compounds are shown in Fig. S1†. Unless otherwise specified, the barriers of 0 K were mainly used in this paper. The reliabilities of B3LYP and G3B3 methods have been verified in the $N_7O^+$ system.[11] All quantum chemistry calculations were carried out using the Gaussian 09 program package.[20]

The specific impulse and chamber combustion temperature were estimated by NASA's CEA code.[21,22] The equilibrium composition, heat, phase and velocity were supposed during expansion of combustion products from an infinite area combustor. The exhaust gases expand from chamber to exit. The chamber and exit pressures were set to 70 and 1 atm, respectively.

The detonation velocity and pressure were calculated by Kamlet-Jacobs equation for CHNO explosives.[10] For more detail on this equation, see ESI†.

## Results and discussion

### A. Potential energy surfaces around 4-carbonic-$CN_6O$

The isomerization and dissociation pathways of carbonyl diazide (**1** and **2**) are shown in Fig. 2. The oxygen is attached to the central carbon atom, and the two azido ligands point either in the same direction as the oxygen in **1** (*syn-syn*), or one in the same direction and the other one in the opposite direction in **2** (*syn-anti*). **1** lies 1.7 kcal $mol^{-1}$ below **2**, and isomerization barrier for conversion **2** to **1** is 7.4 kcal $mol^{-1}$. The computational results are consistent with the previous investigations.[5-7,23,24] According to the references 6, 7, 23 and 24, *anti–anti* carbonyl diazide is rather unstable and was not involved in further consideration.

There are two pathways for the dissociation of **1** to cyanogen azide ($NCN_3$, **9)** and nitrous oxide ($N_2O$, **12)**: one is stepwise, and the other one is concerted. The stepwise pathway involves an intermediate (**3**, *z*-5-azido-oxatriazole) with a five-membered ring. The first step is cyclization of **1** to **3** with a barrier of 25.0 kcal $mol^{-1}$, and the second step is dissociation of **3** to **9** and **12** with a barrier of 39.1 kcal $mol^{-1}$. The intermediate **3** is located in a potential well and its isomerization barrier to **1** is only 0.9 kcal $mol^{-1}$. **3** lies 1.3 kcal $mol^{-1}$ above **4 (***e*-5-azido-oxatriazole), and the isomerization via **TS9** crosses a barrier of 5.5 kcal $mol^{-1}$. It tends to isomerize rather than dissociate because the barrier of isomerization to **1** is lower than that of dissociation to **9** and **12** by 38.2 kcal $mol^{-1}$. The concerted pathway involving only one transition state with a four-membered ring, **TS2**, has a very high barrier of 90.9 kcal $mol^{-1}$. At the insight of synthesis, **1** can be formed by **9** and **12**, and the pathway *via* **TS3** crosses a barrier of 35.7 kcal $mol^{-1}$.

For the dissociation of **2** to **9** and **12,** there are also two similarly pathways. The concerted pathway involving **TS7** crosses a barrier of 88.2 kcal $mol^{-1}$. The stepwise pathway involving an intermediate (**4**) crosses a barrier of 22.7 kcal $mol^{-1}$ at the first step and 42.1 kcal $mol^{-1}$ at the second step. **4** tends to isomerize to **2** with a barrier of 1.6 kcal $mol^{-1}$. There are another possible pathways for the decomposition of **2** to $OCN_4$ (**10**) and $N_6$ (**11**). **2** decomposes to **10** with evolution of $N_2$ (**13**) *via* **TS8**. It undergoes break of the α-N-β-N bond on one side and an azide group shifts from carbonyl to α-N on the other side with a barrier of 31.6 kcal $mol^{-1}$. The isomerization of **2** to **5** involving attachment of α-N of an azide group to γ-N of the other azide group *via* **TS6** crosses a barrier of 39.4 kcal $mol^{-1}$. **5** transfers to **7** (*z*-1-azido-2-isocyanatodiazene) with a barrier of 1.0 kcal $mol^{-1}$. The dissociation of **7** can proceed along three different pathways:

(1) dissociation to **10** and **13** via **TS15** crossing a barrier of 18.2 kcal $mol^{-1}$; transformation to **8** with a barrier of 9.7 kcal $mol^{-1}$ and dissociation of **8** to **10** and **13** with a barrier of 2.5 kcal $mol^{-1}$; (2) dissociation to **11** ($N_6$) and **14** (CO) via **TS16** crossing a barrier of 44.3 kcal $mol^{-1}$. (3) **2** cyclizes to **4**, then **4** isomerizes to **6** (tetrazolo[1,5-d][1,2,3,4]oxatriazole) *via* **TS11** with a barrier of 31.3 kcal $mol^{-1}$, but the total barrier from **2** to **TS11** is 52.4 kcal $mol^{-1}$. Accordingly, it is not an optimum pathway for isomerization of **1** or **2** to **6**. The dissociation of **6** to **10** and **13** *via* **TS14** crosses a barrier of 46.0 kcal $mol^{-1}$. **6** can also isomerize to **5** *via* **TS13** crossing a barrier of 6.2 kcal $mol^{-1}$, and **5** decomposes to **10** or **11** ultimately.

Although **1** is thermodynamically dominant isomer, its decomposition goes through **2**, and the optimum pathway of decomposition is **1→TS4→2→TS8→C(10+13)** with a maximum barrier of 31.6 kcal $mol^{-1}$ (from **2** to **TS8**). The pathway *via* **TS8** is similar to our previous report on the self-dissociation of $N_7O^+$, and 4-oxo-$N_7O^+$ dissociates to $N_5O^+$ and $N_2$ with a barrier of about 20 kcal $mol^{-1}$. The mechanism also supports the matrix isolation of $OCN_4$ by decomposition of carbonyl diazide experimentally.[25]

**B. Potential energy surfaces around 3-carbonic-$CN_6O$**

The isomerization and dissociation pathways of 3-carbonic-$CN_6O$ (**15**, **16** and **17**) are shown in Fig. 3. The **15**, **16** and **17** are the three possible 3-carbonic isomers, *i.e.*, the oxygen is attached to the central nitrogen atom, and both 3-carbonic and azido ligands point in the same direction as oxygen (**15**), 3-carbonic in the same direction and azido in the opposite direction (**16**), or azido in the same direction and 3-carbonic in the opposite direction (**17**). The isomers **15**, **16** and **17** lie 86.9, 88.5 and 86.7 kcal $mol^{-1}$ above **1**, respectively. The isomerization barriers for conversion of **15** to **16** and **15** to **17** are 21.0 and 5.9 kcal $mol^{-1}$, respectively.

Except for the pathways to **16** and **17**, the dissociation and isomerization of **15** can proceed along six different pathways: (1) a stepwise pathway to $N_2O$ (**12**) and $N_2CN_2$ (**28**) involving an intermediate (**18**) with a five-membered ring crossing a limiting barrier (from **15** to **TS19**) of 13.2 kcal $mol^{-1}$; (2) a pathway to **19** involving the **TS20** transition state with a five-membered ring and a barrier of 26.9 kcal $mol^{-1}$; (3) the formation of a new N-O bond between the 6-N and O *via* **TS21** with a four-membered ring, producing **12** and **28**, and a barrier of 57.0 kcal $mol^{-1}$; (4) the formation of a new N-O bond between the 2-N and O *via* **TS22** with a four-membered ring, producing $N_2O$ (**12**) and $CNN_3$ (isocyanogen azide, **29**) and a barrier of 77.9 kcal $mol^{-1}$; (5) a pathway to **13** and **31** going through a transition state (**TS23**) involving the break of a 5-N-6-N bond and a 3-C approaching to 5-N with a decomposition barrier of 22.8 kcal $mol^{-1}$; (6) a pathway to **13** and **30** going through a transition state (**TS24**) involving the break of a 2-N-3-C bond and a 5-N approaching to 3-C with a decomposition barrier of 14.6 kcal $mol^{-1}$. The optimum pathway of dissociation for **15** is **15→TS19→18→TS25→C(12+28)** with a maximum barrier of 13.2 kcal $mol^{-1}$ (from **15** to **TS19**).

Except for the pathways to **15** and **17**, there are three pathways for the dissociation and isomerization of **16**: (1) a pathway to **19** involving an intermediate (**21**) with a five-membered ring crossing a limiting barrier (from **16** to **TS31**) of 24.2 kcal $mol^{-1}$; (2) a pathway to **24** involving an intermediate (**21**), and a higher barrier *via* **TS38** than *via* **TS37** by 11.9 kcal $mol^{-1}$; (3) the formation of a new N-O bond between the 6-N and O *via* **TS34** with a four-membered ring, producing **12** and **28**, and a barrier of 60.7 kcal $mol^{-1}$. Because the direct dissociation pathway of **16** crosses a higher barrier than that of **15**, the optimum pathway of dissociation for **16** is **16→TS28→15→TS19→18→TS25→C(12+28)**.

Except for the pathways to **15** and **16**, the dissociation and isomerization of **17** can proceed along four pathways: (1) a isomerization pathway to **18** involving an intermediate (**20**) with a five-membered ring crossing a limiting barrier (from **17** to **TS30**) of 12.5 kcal $mol^{-1}$; (2) a isomerization pathway to **23** involving the **TS33** transition state with a five-membered ring, a barrier of 30.0 kcal $mol^{-1}$, and the optimal dissociation of **23** to **13** and **30** crossing a limiting barrier of 12.2 kcal $mol^{-1}$ (from **23** to **TS48**); (3) a pathway to **13** and **31** undergoing a transition state (**TS35**) involving the break of a 5-N-6-N bond and a 3-C approaching to 5-N with a decomposition barrier of 24.4 kcal $mol^{-1}$; (4) a isomerization pathway to **22** involving attachment of 1-N to 3-C via **TS32**, and a barrier of 12.1 kcal $mol^{-1}$. There are six possible pathways for the dissociation and isomerization of **22**: (1) it decomposes to **28** with evolution of **13** via **TS39** with a barrier of 32.5 kcal $mol^{-1}$; (2) it decomposes to ONCN (**32)** with evolution of **13** *via* **TS40** with a barrier of 37.2 kcal $mol^{-1}$; (3) the O shifts from N to C *via* **TS42** with the evolution of **13** and **14** crossing a barrier of 62.2 kcal $mol^{-1}$; (4) the multi-step pathway of decomposition to **13** and **33** goes through two intermediates, **24** (tetrazolo[5,1-d][1,2,3,5]oxatriazole) and **26**, with a limiting barrier (from **24** to **TS46**) of 32.3 kcal $mol^{-1}$; (5) the concerted pathway of isomerization to *z*-4-azido-oxatriazole (**25**) *via* **TS43** crosses a barrier of 20.4 kcal $mol^{-1}$; (6) the stepwise pathway of isomerization to **25** goes through an intermediate (**24**) with a bicyclic five-membered ring crossing a limiting barrier (from **24** to **TS45**) of 11.6 kcal $mol^{-1}$. More details of reaction pathways of 4-azido-oxatriazole, see section E. The optimum pathway of dissociation of **17** is **17→TS30→20→TS36→18→TS25→C(12+28)** with a maximum barrier of 12.5 kcal $mol^{-1}$ (from **17** to **TS30**).

**C. Potential energy surfaces around 2-carbonic-$CN_6O$**

The corresponding pathways of 2-carbonic-$CN_6O$ are shown in Fig. 4. According to the directions of ligands of 4-N as O, there are three 3-carbonic isomers (**34**, **35**, and **36**). **34** lies 0.9 and 1.0 kcal $mol^{-1}$ below **35** and **36**, respectively. The barriers for conversion of **34** to **35** and **34** to **36** are 6.9 and 24.2 kcal $mol^{-1}$, respectively.

Except for the pathways to **35** and **36**, the dissociation and isomerization of **34** can proceed along five different pathways: (1) a stepwise pathway to **9** and **12** involving an intermediate (**37**) with a five-membered ring crossing a limiting barrier (from **34** to **TS50**) of 17.0 kcal $mol^{-1}$; (2) a pathway to **13** and **42** going through a transition state (**TS53**) involving the break of a 5-N-6-N bond and a 3-N approaching to 5-N with a decomposition barrier of 26.2 kcal $mol^{-1}$; (3) the formation of a new N-O bond between the 6-N and O *via* **TS52** with a four-membered ring, producing **9** and **12**, and a barrier of 63.7 kcal $mol^{-1}$; (4) the formation of a new N-O bond between the 2-C and O *via* **TS51** with a four-membered ring, producing **38** ($N_5^+OCN^-$) and a barrier of 62.9 kcal $mol^{-1}$; (5) a pathway to **45** (1-carbonic-$CN_6O$) *via* **TS57** involving the break of 2-C-3-N and formation of a new 2-N-3-N bond with a barrier of 71.8 kcal $mol^{-1}$. The optimum pathway of dissociation for **34** is **34→TS50→37→TS54→C(9+12)** with a maximum barrier of 17.0 kcal $mol^{-1}$ (from **34** to **TS50**).

Except for the pathways to **34** and **36**, the dissociation and isomerization of **35** have two pathways: (1) a pathway to **38** involving a transition state (**TS59**) with a four-membered ring crossing a barrier of 62.2 kcal $mol^{-1}$; (2) a isomerization pathway to **39** involving attachment of 1-N to 5-N via **TS58** crossing a barrier of 18.4 kcal $mol^{-1}$. There exist three possible pathways for the dissociation of **39**: (1) it decomposes to **9** with evolution of **12** *via* **TS64** with a barrier of 13.4 kcal $mol^{-1}$; (2) the O shifts to N which links cyanogen group *via* **TS66**, and **39** dissociates to **13** and

**32** crossing a barrier of 81.7 kcal $mol^{-1}$; (3) a stepwise pathway to **13** and **44** involving an intermediate (**43**), the center N with three arms, and it crosses a limiting barrier (from **39** to **TS67**) of 25.4 kcal $mol^{-1}$. The optimum pathway of dissociation for **35** is **35→TS58→39→TS64→C(9+12)** with a maximum barrier of 18.4 kcal $mol^{-1}$ (from **35** to **TS58**).

Except for the pathways to **34** and **35**, there are four dissociation and isomerization pathways for **36**: (1) an isomerization pathway to **41** involving break of 4-N-5-N bond and attachment of 1-N to 5-N via **TS57** crossing a barrier of 63.4 kcal $mol^{-1}$; (2) a pathway to **9** with evolution of **12** involving a transition state (**TS62**) with a four-membered ring crossing a barrier of 65.2 kcal $mol^{-1}$; (3) a pathway to **13** and **42** undergoing a transition state (**TS63**) involving the break of a 5-N-6-N bond and a 3-N approaching to 5-N crossing a barrier of 28.7 kcal $mol^{-1}$; (4) a stepwise pathway to **9** and **12** involving an intermediate (**40**) with a five-membered ring crossing a limiting barrier (from **36** to **TS60**) of 16.5 kcal $mol^{-1}$ or transformation from **40** to **37** *via* **TS68**. The optimum pathway of dissociation for **36** is **36→TS60→40→TS65→C(9+12)** with a maximum barrier of 16.5 kcal $mol^{-1}$ (from **36** to **TS60**).

**D. Potential energy surfaces around 1-carbonic-$CN_6O$**

The isomerization and dissociation pathways of 1-carbonic-$CN_6O$ are shown in Fig. 5. According to the directions of ligands of 4-N as O, there are three 1-carbonic isomers (**45**, **46**, and **47**). **45** lies 1.6 and 2.1 kcal $mol^{-1}$ below **46** and **47** respectively. The barriers for transformation of **45** to **46** and **45** to **47** are 5.8 and 32.8 kcal $mol^{-1}$, respectively. It is difficult to twist the multi-bond of 3-N-4-N in **47**. Whether forward or reverse, the isomerizations between cyanogen and isocyanogen, such as **34** and **45** in Fig. 4, cross ultra-high barriers exceeding 35 kcal $mol^{-1}$ and these pathways were excluded for further consideration.

Except for the pathways to **46** and **47**, the dissociation and isomerization of **45** can proceed along four different pathways: (1) the stepwise pathway involving an intermediate (**48**) with a five-membered ring, decomposition of **48** via **TS74** (to **12** and **29**) or **TS75** (to **13** and **51**), and crossing a limiting barrier of 17.5 kcal $mol^{-1}$ (from **45** to **TS70**); (2) the stepwise pathway involving an intermediate (**49**) with a linear chain, the isomerization *via* **TS71** with a barrier of 14.1 kcal $mol^{-1}$, and decomposition of **49** *via* **TS76** (to **11** and **14**), **TS77** (to **10** and **13**) or **52** (to **10** and **13**); (3) the formation of a new N-O bond between the 6-N and O *via* **TS72** with a four-membered ring, producing **12** and **29**, and a barrier of 67.2 kcal $mol^{-1}$; (4) a pathway to **13** and **50** going through a transition state (**TS73**) involving the break of a 5-N-6-N bond and a 3-N approaching to 5-N with a decomposition barrier of 25.8 kcal $mol^{-1}$. The optimum pathway of dissociation for **45** is **45→TS71→49→TS95→52→TS87→C(10+13)** with a maximum barrier of 14.1 kcal $mol^{-1}$ (from **45** to **TS71**). There is an entrance for isomerizing **49** (*e*) to **7** (*z*). As shown in Fig. S2†, an energy barrier of 47.5 kcal $mol^{-1}$ needs to be crossed. $N_5^+NCO^-$ (**38**) is not stable, and its transformation to **49** crosses a barrier of not more than 1 kcal $mol^{-1}$, also see Fig. S2†.

Except for the pathways to **45** and **47**, there are two pathways for the dissociation and isomerization of **46**: (1) the stepwise pathway involving an intermediate (**52**, *e*-1-azido-2-isocyanatodiazene) with a linear chain, the isomerization *via* **TS80** with a barrier of 13.2 kcal $mol^{-1}$, and decomposition of **52** *via* **TS86** (to **11** and **14**) or **TS87** (to **10** and **13**); (2) a isomerization pathway to **53** involving attachment of 3-N to 7-N via **TS81**, and a barrier of 20.8 kcal $mol^{-1}$. There are four possible pathways for the dissociation and isomerization of **53**: (1) it decomposes to **33** with evolution of **13** *via* **TS88** with a barrier of 14.1 kcal $mol^{-1}$; (2) it decomposes to **29** with evolution of **12** *via* **TS89** with a barrier of 43.9 kcal $mol^{-1}$; (3) the O shifts

to N which links isocyanogen group *via* **TS91** with the formation of **56** crossing a barrier of 78.5 kcal $mol^{-1}$, and **56** dissociates to **13** and **33** with a barrier of 4.1 kcal $mol^{-1}$; (4) a stepwise pathway to **13** and **57** involving an intermediate (**55**), the center N with three arms, and it crosses a limiting barrier (from **53** to **TS92**) of 24.3 kcal $mol^{-1}$. The optimum pathway of dissociation for **46** is **46→TS80→52→TS87→C(10+13)** with a maximum barrier of 13.2 kcal $mol^{-1}$ (from **46** to **TS80**).

Except for the pathways to **45** and **46**, The dissociation of **47** exists four pathways: (1) a stepwise pathway to **12** and **29** involving an intermediate (**54**) with a five-membered ring crossing a limiting barrier (from **47** to **TS82**) of 16.1 kcal $mol^{-1}$; (2) a decomposition pathway to **9** and **12** involving break of 4-N-5-N bond and attachment of 1-C to 5-N via **TS83** crossing a barrier of 26.2 kcal $mol^{-1}$; (3) a pathway to **29** with evolution of **12** involving a transition state (**TS84**) with a four-membered ring crossing a barrier of 67.0 kcal $mol^{-1}$; (4) a pathway to **13** and **50** going through a transition state (**TS85**) involving the break of a 5-N-6-N bond and a 3-N approaching to 5-N crossing a barrier of 22.1 kcal $mol^{-1}$. The optimum pathway of dissociation for **47** is **47→TS82→54→TS90→C(12+29)** with a maximum barrier of 16.1 kcal $mol^{-1}$ (from **47** to **TS82**).

**E. Potential energy surfaces around 4-azido-oxatriazole**

The isomerization and dissociation pathways of **25** are shown in Fig. 3 and Fig. 6. The pathway of **25** to **22** has been discussed in Section B already. **25** can produce **9** with evolution of **12** ($N_2O$) or **60** (NON). The barrier of formation of **9** and **12** is 35.5 kcal $mol^{-1}$, while the formation of **9** and **60** crosses a higher barrier of 117.8 kcal $mol^{-1}$. The isomerization from **25** to **58** crosses a barrier of 4.5 kcal $mol^{-1}$, and their energies are almost the same. The **58** has two similar decomposition pathways *via* **TS100** and **TS101**, and the barriers are 34.2 and 119.7 kcal $mol^{-1}$, respectively. Unlike **25**, **58** can decompose to **13** and **30** via **TS102** with a barrier of 13.3 kcal $mol^{-1}$. Another pathway for isomerization of **58** is the formation of **59** with bicyclic five-membered ring. The barrier for opening the ring is only 5.7 kcal $mol^{-1}$. **59** can break the N-O and C-N bonds *via* **TS103** with a barrier of 43.7 kcal $mol^{-1}$, and form a three arms isomer (**43**). **43** dissociates to **13** and **44** crossing a barrier of 8.8 kcal $mol^{-1}$. The pathway from **59** to **61** with the break of the C-N and N-N bonds crosses a barrier of 55.3 kcal $mol^{-1}$. The breaks of the C-N bond and the other N-N bond form an intermediate (**62**) with a barrier of 62.0 kcal $mol^{-1}$. **62** decomposes to **13** and **32** *via* **TS106** crossing a barrier of 11.0 kcal $mol^{-1}$. The optimum pathway of dissociation for **25** is **25→TS96→58→TS102→C(13+30)** with a maximum barrier of 13.3 kcal $mol^{-1}$ (from **58** to **TS102**).

**F. Energy barrier, enthalpy of formation and performance**

In this study, the potential energy surfaces of $CN_6O$ have been calculated intensively. Many isomers and conversion mechanisms were acquired. We can extract five noticeable kinds of $CN_6O$ isomers from the potential energy surfaces. (1) W-shaped $CN_6O$ (oxygen atom fixed beyond the 4-position), such as **1** (4-carbonic), **15** (3-carbonic), **34** (2-carbonic) and **45** (1-carbonic). The dissociation pathway of **1**, undergoing evolution of $N_2$ and shift of azide group, crosses a barrier of 31.3 kcal $mol^{-1}$ at G3B3 level. The dissociations of **15**, **34** and **45** go through the transition states with the five-membered rings, and the barriers at G3B3 level are 14.5, 19.1 and 13.8 kcal $mol^{-1}$, respectively. (2) Azido-oxatriazole, such as **3** (5-) and **25** (4-). **3** isomerizes to **1** with a very low barrier of 1.2 kcal $mol^{-1}$ at G3B3 level. **25** should transfer to its *e*-isomer (**58**), and the decomposition barrier from **58** to **TS102** is 13.5 kcal $mol^{-1}$ at G3B3 level. If **25** can form a solid state with strong lattice interaction, the conversion to **58** will be avoided. The decomposition barrier should rise to about 35 kcal $mol^{-1}$ (from **25** to **TS98**). The reaction between oxime groups is a probable pathway for the synthesis of **25**. (3) Azido-diazene, such as **7** and **23**. The

dissociations of **7** and **23** with evolution of dinitrogen cross the barriers of 7.9 (from **7** to **TS17**) and 10.3 (from **23** to **TS48**) kcal $mol^{-1}$ at G3B3 level, respectively. (4) Tetrazolo oxatriazole, such as **6**, **24**, and **59**. The barriers for opening the rings are 8.7, 10.1 and 6.4 kcal $mol^{-1}$ at G3B3 level, respectively. (5) Oxo-pentazole, such as **39** and **53**. The dissociations of **39** and **53** with evolution of $N_2O$ cross the barriers of 16.6 and 16.4 kcal $mol^{-1}$ at G3B3 level, respectively.

The optimum conversion barriers and enthalpies of formation for aforementioned $CN_6O$ isomers are shown in Fig. 7. The detailed pathways for dissociations and their barriers at B3LYP and G3B3 levels are presented in Table S1†. The detailed standard enthalpies of formation in gas phase are presented in Table S2†. Compared with 111.4 (G2), 113.9 (G3) and 109.2 (G4) kcal $mol^{-1}$,[7] the enthalpy of formation of **1** is 115.7 kcal $mol^{-1}$ at B3LYP level, and 110.0 kcal $mol^{-1}$ at G3B3 level. **1** possesses the highest limiting barrier and lowest enthalpy of formation. Although the other isomers contain more enthalpies, they cannot reach the kinetic stability of **1**. The frontier orbital energies of $CN_6O$ isomers provided in Table S3† show that **1** impart the maximum gap between LUMO (lowest unoccupied molecular orbital) and HOMO (highest occupied molecular orbital). It demonstrates the stability of **1** from another viewpoint. The result, shown in Fig. 7, is not a strong inverse correlation between barrier and enthalpy. **53** possesses a very high enthalpy of formation (about 220 kcal $mol^{-1}$), but not a lowest limiting barrier. Except for **1**, the barrier of **34** is relatively high (about 20 kcal $mol^{-1}$).

The relationship between enthalpy of formation and rocket performance for $CN_6O$ is presented in Fig. 8. More detailed data for rocket performances of $CN_6O$ is shown in Table S4†. The enthalpies of formation and rocket performances of comparative set, TNT, RDX, HMX, CL-20 (hexanitrohexaazaisowuritane) and FTDO ([1,2,5]oxadizolo[3,4-4][1,2,3,4]tetrazine-4,6-di-N-dioxide), are shown in Table S5†. With the increase of enthalpy of formation of $CN_6O$, both specific impulse and combustion temperature tend to increase simultaneously. But the growths become slow in the high enthalpy area. If the condensed energy is taken into account, the specific impulse of carbonyl diazide is in the range of 252.3-270.7 s. It is close to those of RDX (267.7 s), HMX (267.5 s) and CL-20 (272.6 s), and much higher than that of TNT (208.6 s). When a $CN_6O$ compound has a 140 kcal $mol^{-1}$ enthalpy of formation, its specific impulse will get to the level of FTDO (297.0 s), which keeps the record of theoretical specific impulse as known CHNO compound.[26] Our previous study on the FTDO indicated that its limiting barrier for decomposition is only 13 kcal $mol^{-1}$ at B3LYP/cc-pVDZ level.[27] The enthalpies of formation of **23**, **25** and **34** are at 190, 140 and 170 kcal $mol^{-1}$ levels, respectively, and the corresponding specific impulses are 332.2, 295.8 and 318.5 s. If **53** is an existing compound, its specific impulse will amazingly reach the level of 350 s. The low chamber combustion temperature can enhance sustainability of working of rocket engine, but $CN_6O$ system must pay a higher combustion temperature than RDX, HMX, CL-20 and FTDO at the same levels of specific impulses.

To calculate the detonation performances of $CN_6O$, the densities were deduced by molecular volumes inside a contour of 0.003 electrons $Bohr^{-3}$ density and 73.6% space occupancy (the unit cell volume per molecule divided by isolated molecular volume for **1**). As shown in Table S6†, the upper and lower limits are 1.817 and 1.644 g $cm^{-3}$, respectively. The detonation performances of $CN_6O$ are presented in Fig. 9. The densities and detonation performances of comparative set are shown in Table S7†. With the increase of enthalpy of formation and density, the detonation velocity and pressure of $CN_6O$ tend to increase. The detonation velocity of carbonyl diazide is

greater than that of TNT (6997 m $s^{-1}$) by about 1000 m $s^{-1}$, but it is much less than those of RDX (8872 m $s^{-1}$), HMX (9191 m $s^{-1}$), CL-20 (9414 m $s^{-1}$) and FTDO (9309 m $s^{-1}$). Only if the enthalpy of formation exceeds 200 kcal $mol^{-1}$, and the density reaches to the upper limit, the detonation velocity and pressure of $CN_6O$ will be greater than CL-20. It can be easily understood by comparing FTDO with CL-20. Although the specific impulse of FTDO is superior to that of CL-20, the detonation velocity and pressure of FTDO are inferior to those of CL-20, because the detonation performances are sensitive to density (1.850 g $cm^{-3}$ FTDO *versus* 1.970 g $cm^{-3}$ CL-20). Compared with CL-20, $CN_6O$ isomers as explosives have little advantage.

## Conclusions

The study on potential energy surfaces of ground state $CN_6O$ demonstrates that carbonyl diazide has the same dissociation mechanism as 4-oxo-$N_7O^+$, the predictive pathway supports the matrix isolation of $OCN_4$, the dissociation barrier is about 30 kcal $mol^{-1}$, and its isomers have more energy contents but lower decomposition barriers. Except for carbonyl diazide, no isomer of $CN_6O$ has a higher barrier than 20 kcal $mol^{-1}$, just as the linear $CN_6O$ isomers have low barriers as their isoelectronic 1-oxo-$N_7O^+$. The specific impulse of carbonyl diazide is near to those of RDX, HMX and CL-20. The W-shaped 2-cabonic-$CN_6O$ crosses a decomposition barrier of 19.1 kcal $mol^{-1}$ at G3B3 level, and its specific impulse is greater than that of carbonyl diazide by about 60 s. The dissociation barrier of 4-azido-oxatriazole is 13.5 kcal $mol^{-1}$ at G3B3 level which is significantly lower than that of carbonyl diazide but same as that of FTDO, and its specific impulse is comparable to FTDO. As a result, the isomers of carbonyl diazide can win the specific impulse but lose the stability. It will be great challenge for synthesis and storage. The explosives need long-term preservation and adapt to various environment. The requirement for stability of rocket fuels, by contrast, is not so severe. The rocket engine can be loaded with fuel at the launch site, and the fuel can maintain stability with external conditions. Another obstacle is relatively high combustion temperature for structural materials of rocket engine. The perspective for $CN_6O$ isomers as explosives is not bright, because they impart low density and instability. The polymeric $(CN_6O)_n$ ($n \geq 2$) may increase the density, and additives may partly improve the stability. We have revealed the nature of $CN_6O$, and further experimental work will be required to identify the theoretical prediction.

## Acknowledgements

The work was partially supported by the National Natural Science Foundation of China (Nos. 51171046, 21303133 and 21403162).

## Notes and references

1 K. O. Christe, R. Haiges, W. W. Wilson and J. A. Boatz, *Inorg. Chem.*, 2010, **49**, 1245.
2 W. Kesting, *Ber. Dtsch. Chem. Ges.*, 1924, **57B**, 1321.
3 T. Curtius and A. Bertho, *Ber. Dtsch. Chem. Ges.*, 1926, **59B**, 565.
4 K. Banert, Y.-H. Joo, T. Rüffer, B. Walfort and H. Lang, *Angew. Chem. Int. Ed.*, 2007, **46**, 1168.
5 X. Zeng, M. Gerken, H. Beckers and H. Willner, *Inorg. Chem.*, 2010, **49**, 9694.
6 A. M. Nolan, B. K. Amberger, B. J. Esselman, V. S. Thimmakondu, J. F. Stanton, R. C. Woods and R. J. McMahon, *Inorg. Chem.*, 2012, **51**, 9846.
7 D. W. Ball, *Comput. Theor. Chem.*, 2011, **965**, 176.

8 H. Shekhar, *Cent. Eur. J. Energ. Mat.*, 2012, **9**, 39.
9 Wikipedia entry on Tsiokovsky rocket equation.
10 M. J. Kamlet and S. J. Jacobs, *J. Chem. Phys.*, 1968, **48**, 23.
11 T. Yu, Y.-Z. Liu, R. Haiges, K. O. Christe, W.-P. Lai and Bo Wu, *RSC Adv.*, 2014, **4**, 28377.
12 A. D. Becke, *J. Chem. Phys*., 1993, 98, 5648.
13 C. Lee, W. Yang, and R. G. Parr, *Phys. Rev. B: Condens. Matter Matter. Phys.*, 1988, **37**, 785.
14 T. H. Dunning Jr, *J. Chem. Phys.*, 1989, **90**, 1007.
15 C. Gonzalez and H. B. Schlegel, *J. Chem. Phys.*, 1989, **90**, 2154.
16 C. Gonzalez and H. B. Schlegel, *J. Chem. Phys.*, 1991, **95**, 5853.
17 A. G. Baboul, L. A. Curtiss, P. C. Redfern and K. Raghavachari, *J. Chem. Phys.*, 1999, **110**, 7650.
18 L. A. Curtiss, K. Raghavachari, P. C. Redfern, V. Rassolov and J. A. Pople, *J. Chem. Phys.*, 1998, **109**, 7764.
19 webbook.nist.gov/chemistry
20 M. J. Frisch, G. W. Trucks, H. B. Schlegel, G. E. Scuseria, M. A. Robb, J. R. Cheeseman, G. Scalmani, V. Barone, B. Mennucci, G. A. Petersson, H. Nakatsuji, M. Caricato, X. Li, H. P. Hratchian, A. F. Izmaylov, J. Bloino, G. Zheng, J. L. Sonnenberg, M. Hada, M. Ehara, K. Toyota, R. Fukuda, J. Hasegawa, M. Ishida, T. Nakajima, Y. Honda, O. Kitao, H. Nakai, T. Vreven, J. A. Montgomery, Jr., J. E. Peralta, F. Ogliaro, M. Bearpark, J. J. Heyd, E. Brothers, K. N. Kudin, V. N. Staroverov, R. Kobayashi, J. Normand, K. Raghavachari, A. Rendell, J. C. Burant, S. S. Iyengar, J. Tomasi, M. Cossi, N. Rega, J. M. Millam, M. Klene, J. E. Knox, J. B. Cross, V. Bakken, C. Adamo, J. Jaramillo, R. Gomperts, R. E. Stratmann, O. Yazyev, A. J. Austin, R. Cammi, C. Pomelli, J. W. Ochterski, R. L. Martin, K. Morokuma, V. G. Zakrzewski, G. A. Voth, P. Salvador, J. J. Dannenberg, S. Dapprich, A. D. Daniels, O. Farkas, J. B. Foresman, J. V. Ortiz, J. Cioslowski and D. J. Fox, *Gaussian 09, Revision B. 01*, Gaussian, Inc., Wallingford CT, 2009.
21 S. Gordon and B. J. McBride, *Computer program for calculation of complex chemical equilibrium compositions and applications. I. Analysis*, NASA, 1994.
22 B. J. McBride and S. *Gordon, Computer program for calculation of complex chemical equilibrium compositions and applications. II. User's manual and program description*, NASA, 1996.
23 B. Napolion, J. D. Watts, M.-J. Huang, F. M. McFarland, E. E. McClendon, W. L. Walters and Q. L. Williams, *Chem. Phys. Lett.*, 2013, **559**, 18.
24 B. K. Amberger, B. J. Esselman, R. C. Woods and R. J. McMahon, *J. Mol. Spectrosc.*, 2014, **295**, 15.
25 X. Zeng, M. Gerken, H. Beckers and H. Willner, *Angew. Chem. Int. Ed.*, 2011, **50**, 482.
26 D. Lempert and A. Shastin, *Triazines as a basis for new energetic compounds creation*, Lecture in Xi'an Modern Chemistry Research Institute, May 20th, 2014, Prof. Lempert's e-mail: lempert@icp.ac.ru.
27 W.-P. Lai, P. Lian, T. Yu, J.-H. Bu, Y.-Z. Liu, W.-L. Zhu, J. Lv and Z.-X. Ge, *J. Mol. Model.*, 2014, **20**, 2343.

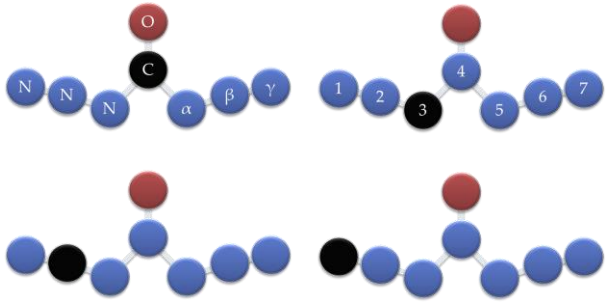


**Fig. 1** W-shaped $CN_6O$. The oxygen atom fixed beyond the central position and carbon atom at different positions.

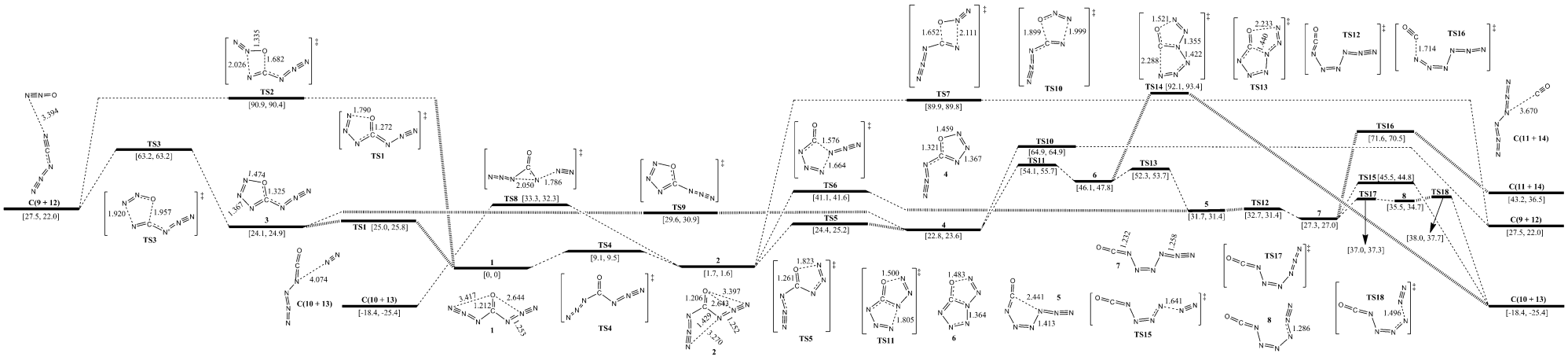


**Fig. 2** Schematic potential energy surfaces around 4-carbonic-$CN_6O$ (carbonyl diazide) at the B3LYP/aug-cc-pVDZ level. Gibbs free energies at 0 K (former) and 298 K (latter) are in brackets. The energy scales are offset to 0 kcal $mol^{-1}$ for *syn-syn* carbonyl diazide as the reference. The crucial bond lengths are labeled in angstroms.

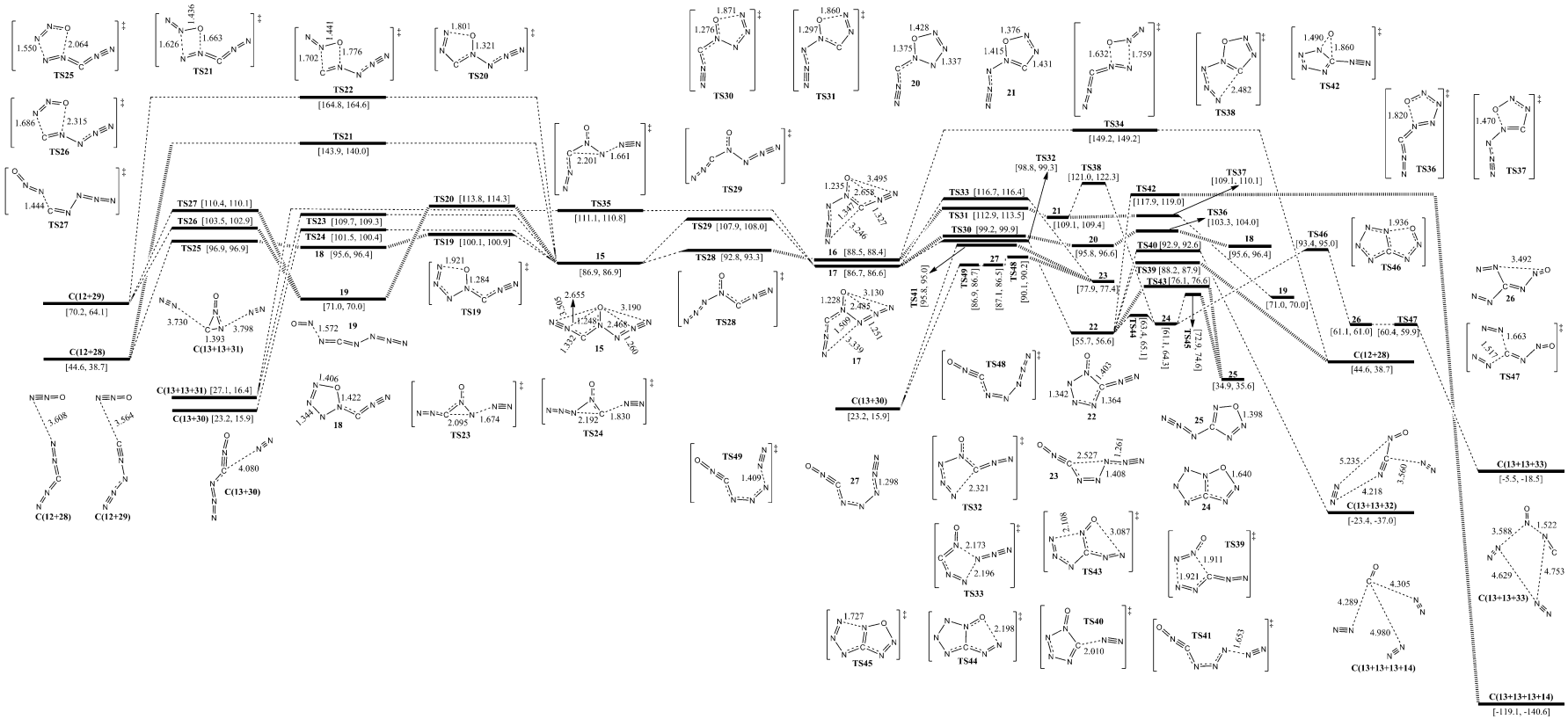

**Fig. 3** Schematic potential energy surfaces around 3-carbonic-$CN_6O$ at the B3LYP/aug-cc-pVDZ level. Gibbs free energies at 0 K (former) and 298 K (latter) are in brackets. The energy scales are offset to 0 kcal $mol^{-1}$ for *syn-syn* carbonyl diazide as the reference. The crucial bond lengths are labeled in angstroms.

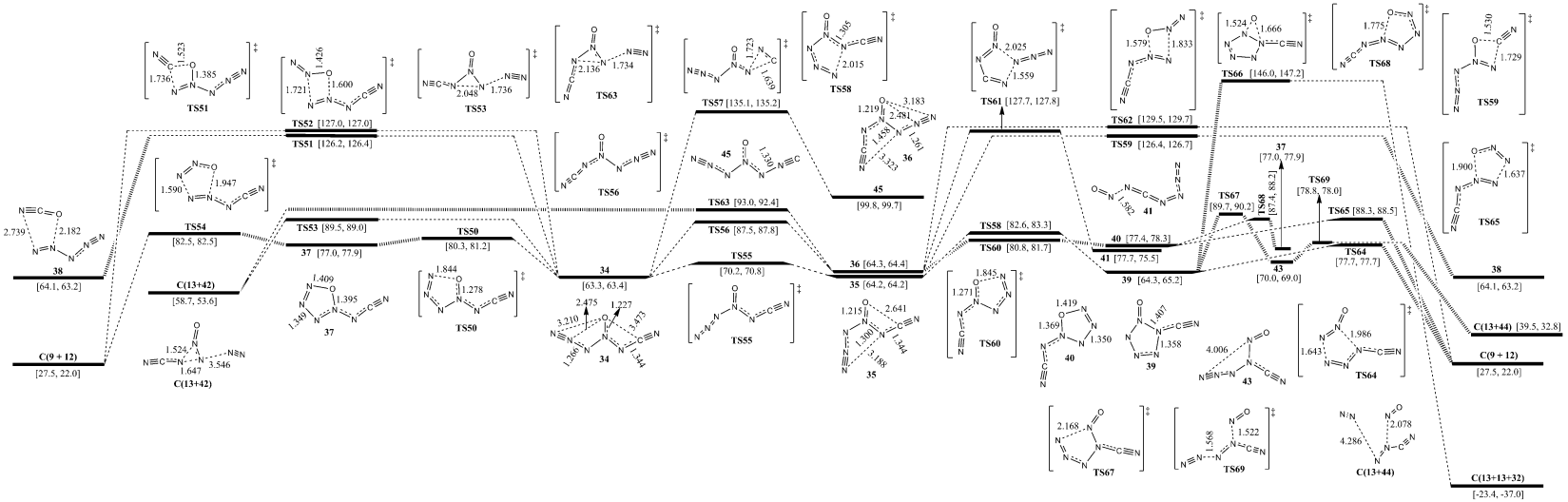

**Fig. 4** Schematic potential energy surfaces around 2-carbonic-$CN_6O$ at the B3LYP/aug-cc-pVDZ level. Gibbs free energies at 0 K (former) and 298 K (latter) are in brackets. The energy scales are offset to 0 kcal $mol^{-1}$ for *syn-syn* carbonyl diazide as the reference. The crucial bond lengths are labeled in angstroms.

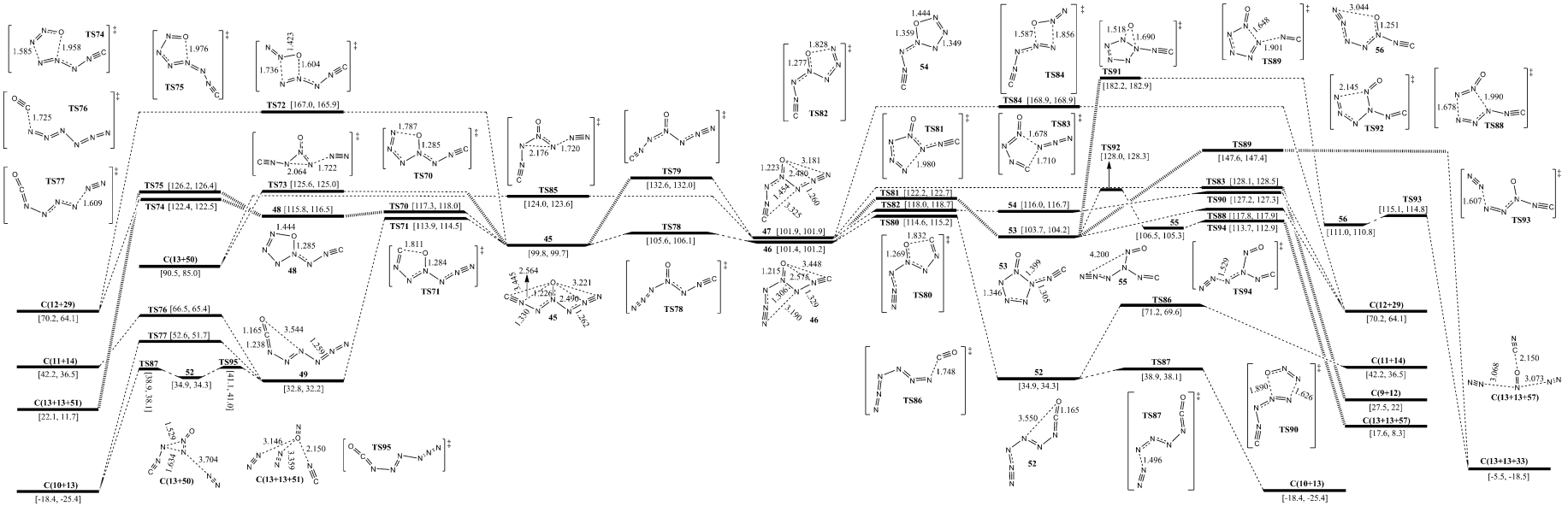

**Fig. 5** Schematic potential energy surfaces around 1-carbonic-$CN_6O$ at the B3LYP/aug-cc-pVDZ level. Gibbs free energies at 0 K (former) and 298 K (latter) are in brackets. The energy

scales are offset to 0 kcal mol$^{-1}$ for *syn-syn* carbonyl diazide as the reference. The crucial bond lengths are labeled in angstroms.

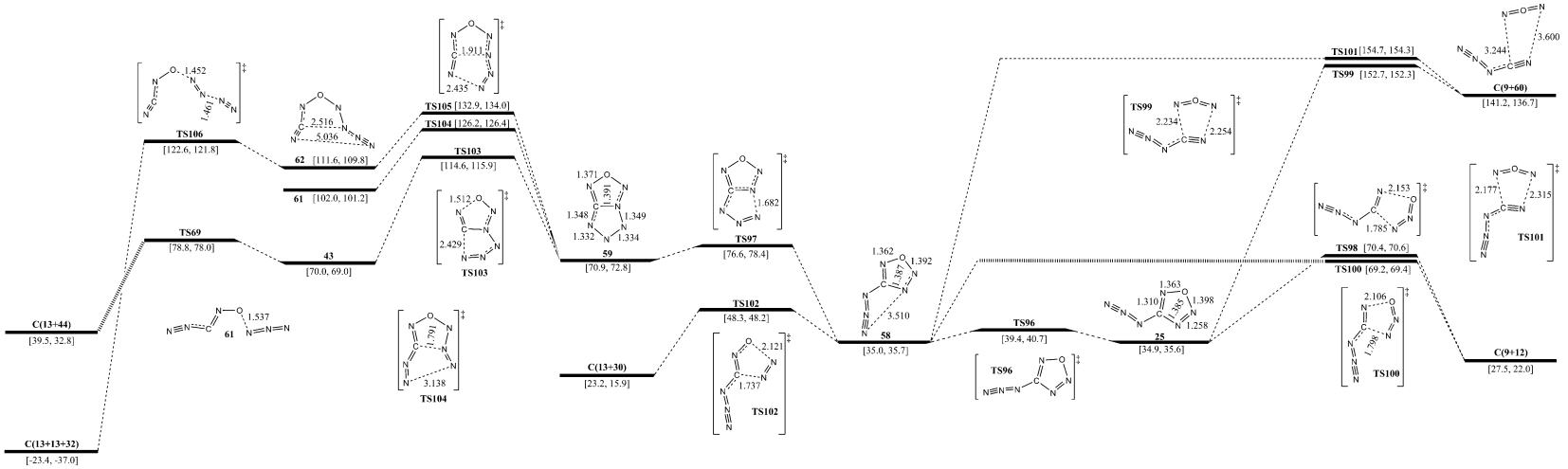


**Fig. 6** Schematic potential energy surfaces around 4-azido-oxatriazole at the B3LYP/aug-cc-pVDZ level. Gibbs free energies at 0 K (former) and 298 K (latter) are in brackets. The energy scales are offset to 0 kcal mol$^{-1}$ for *syn-syn* carbonyl diazide as the reference. The crucial bond lengths are labeled in angstroms.

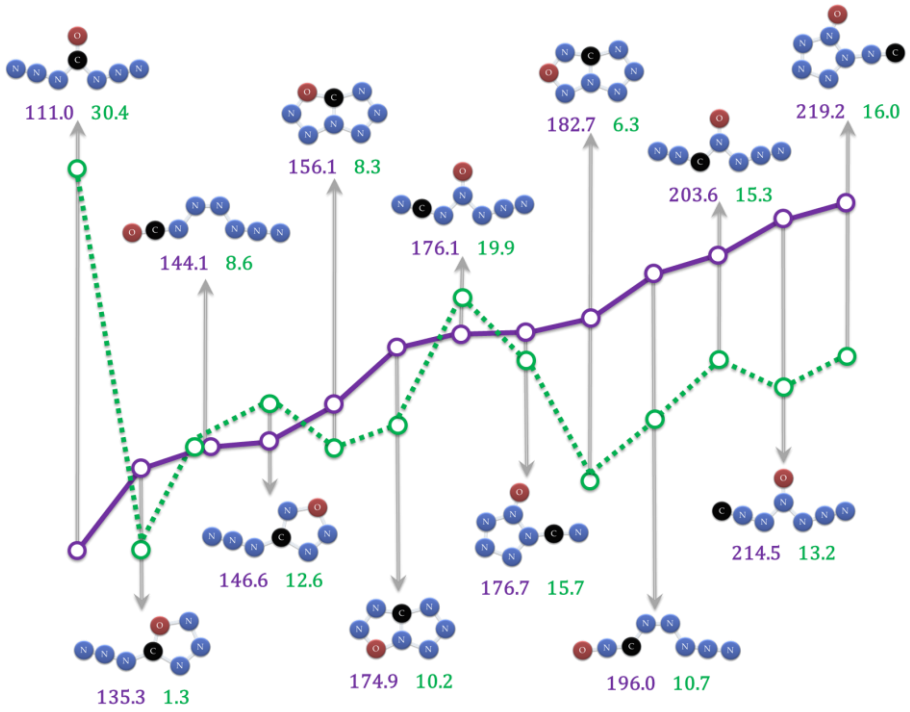


**Fig. 7** Optimum conversion barriers *versus* enthalpies of formation for different isomers of $CN_6O$ at G3B3 level and 298.15 K in kcal $mol^{-1}$. The activation free energy barriers are in green and dot line. The enthalpies of formation are in purple and solid line.

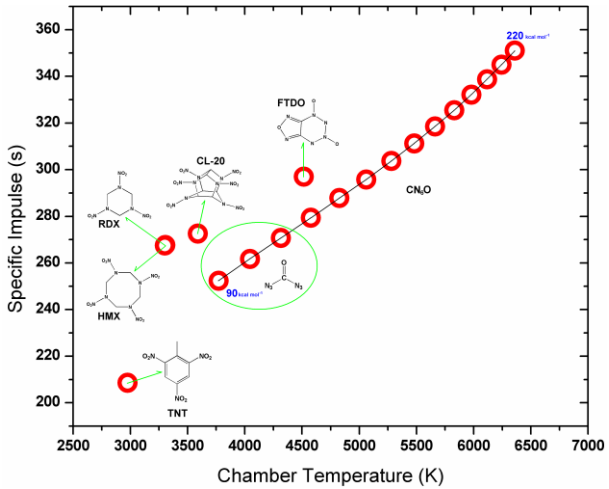


**Fig. 8** Specific impulses for TNT, RDX, HMX, CL-20, FTDO and $CN_6O$ *versus* their chamber combustion temperatures. The enthalpies of formation of $CN_6O$ from 90 to 220 kcal $mol^{-1}$ with an interval of 10 kcal $mol^{-1}$.

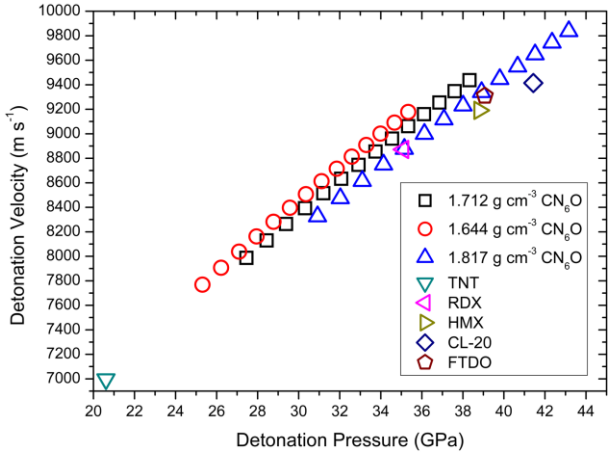


**Fig. 9** Detonation velocities for TNT, RDX, HMX, CL-20, FTDO and $CN_6O$ *versus* their detonation pressure. The enthalpies of formation of $CN_6O$ from 90 to 220 kcal $mol^{-1}$ with an interval of 10 kcal $mol^{-1}$.